10. **Guyton AC, Jones CE, and Coleman TG.** *Circulatory Physiology: Cardiac Output and Its Regulation, 2nd ed.* Philadelphia: WB Saunders, 1973, p. 263-284.

11. **Lee RW, and Goldman S.** Mechanism for decrease in cardiac output with atrial natriuretic peptide in dogs. *Am J Physiol Heart Circ Physiol* 256: H760-H765, 1989.

12. **Little WC, Ohno M, Kitzman DW, Thomas JD, and Cheng CP.** Determination of left ventricular chamber stiffness from the time for deceleration of early left ventricular filling. *Circulation* 92: 1933-1939, 1995.

13. **Lucas C, Johnson W, Hamilton MA, Fonarow GC, Woo MA, Flavell CM, Creaser JA, and Stevenson LW.** Freedom from congestion predicts good survival despite previous class IV symptoms of heart failure. *Am Heart J* 140: 840-847, 2000.

14. **Mandinov L, Eberli FR, Seiler C, and Hess OM.** Diastolic heart failure. *Cardiovasc Res* 45: 813-825, 2000.

15. **Maughan WL, Shoukas AA, Sagawa K, and Weisfeldt ML.** Instantaneous pressure-volume relationship of the canine right ventricle. *Circ Res* 44: 309-315, 1979.

16. **McGee SR.** Physical examination of venous pressure: a critical review. *Am Heart J* 136: 10-18, 1998.

17. **Ogilvie RI, and Zborowska-Sluis D.** Effect of chronic rapid ventricular pacing on total vascular capacitance. *Circulation* 85: 1524-1530, 1992.

18. **Ohno M, Cheng CP, and Little WC.** Mechanism of altered patterns of left ventricular filling during the development of congestive heart failure. *Circulation* 89: 2241-50, 1994.

19. **Pouleur H, Covell JW, and Ross J Jr.** Effects of nitroprusside on venous return and central blood volume in the absence and presence of acute heart failure. *Circulation* 61: 328-337, 1980.

20. **Sagawa K, Maughan WL, Suga H, and Sunagawa K.** *Cardiac Contraction and*

Pressure-Volume Relationship. Oxford, UK: Oxford Univ. Press, 1988, p. 232-298.

21. **Sarnoff SJ, and Berglund E.** Ventricular function. 1. Starling's law of the heart, studied by means of simultaneous right and left ventricular function curves in the dog. *Circulation* 9: 706-718, 1953.
22. **Shoukas AA.** Carotid sinus baroreceptor reflex control and epinephrine. Influence on capacitive and resistive properties of the total pulmonary vascular bed of the dog. *Circ Res* 51: 95-101, 1982.
23. **Stevenson LW, Tillisch JH, Hamilton M, Luu M, Chelimsky-Fallick C, Moriguchi J, Kobashigawa J, and Walden J.** Importance of hemodynamic response to therapy in predicting survival with ejection fraction less than or equal to 20% secondary to ischemic or nonischemic dilated cardiomyopathy. *Am J Cardiol* 66: 1348-1354, 1990.
24. **Stone HL, Bishop VS, and Dong EJ.** Ventricular function in cardiac denervated and cardiac sympathectomized conscious dogs. *Circ Res* 20: 587-593, 1967.
25. **Suga H, and Sagawa K.** Instantaneous pressure-volume relationships and their ratio in the excised, supported canine left ventricle. *Circ Res* 35: 117-126, 1974.
26. **Sunagawa K, Maughan WL, Burkhoff D, and Sagawa K.** Left ventricular interaction with arterial load studied in isolated canine ventricle. *Am J Physiol Heart Circ Physiol* 245: H773-H780, 1983.
27. **Sunagawa K, Sagawa K, and Maughan WL.** Ventricular interaction with the loading system. *Ann Biomed Eng* 12: 163-189, 1984.
28. **Todaka K, Leibowitz D, Homma S, Fisher PE, Derosa C, Stennett R, Packer M, and Burkhoff D.** Characterizing ventricular mechanics and energetics following repeated coronary microembolization. *Am J Physiol Heart Circ Physiol* 272: H186-H194, 1997.
29. **Uemura K, Sugimachi M, Kawada T, Kamiya A, Jin Y, Kashihara K, and Sunagawa K.**

A novel framework of circulatory equilibrium. *Am J Physiol Heart Circ Physiol* 286; H2376-H2385, 2004.

30. **Ursino M.** Interaction between carotid baroregulation and the pulsating heart: a mathematical model. *Am J Physiol* 275: H1733-H1747, 1998.

31. **Vatner SF, and Braunwald E.** Cardiovascular control mechanisms in the conscious state. *N Engl J Med* 293: 970-976, 1975.

32. **Wagner JG, and Leatherman JW.** Right ventricular end-diastolic volume as a predictor of the hemodynamic response to a fluid challenge. *Chest* 113: 1048-1054, 1998.

LEGENDS

Fig. 1. Diagram of circulatory equilibrium for cardiac output (CO), venous return (CO_V), left atrial pressure (P_{LA}), and right atrial pressure (P_{RA}). The equilibrium CO, P_{LA} and P_{RA} are obtained as the intersection point of the venous return surface and the integrated cardiac output curve [modified from Uemura et al. (Ref. 29)].

Fig. 2. Changes in arterial pressure, CO, P_{LA} and P_{RA} throughout the examination. As P_{RA} and P_{LA} decreases following stepwise reduction of the stressed blood volume, CO also decreases (Frank-Starling mechanism).

Fig. 3. The relationship between CO and P_{LA} (A), and between CO and P_{RA} (B) in a single dog. Thin solid lines represent the best fit curves of the 3-parameter logarithmic functions obtained by the least square method.

Fig. 4. Cardiac output curves for a single animal under normal and left ventricular failure conditions for the left heart (A) and the right heart (B). ●, reference hemodynamic values under normal conditions; ■, reference hemodynamic values under left ventricular failure; ○, measured points under normal conditions; □, measured points under left ventricular failure conditions. Estimated cardiac output curves under normal conditions (solid lines) and under left ventricular failure conditions (dashed lines) accurately correspond with the measured points.

Fig. 5. Relationship between estimated and measured values of CO for the left heart (A), and the right heart (B) for 104 steps pooled over 13 output curves. ●, normal cardiac function; ○, left

heart failure; dashed line, lines of identity. Regression analysis (solid line) reveals that estimated *CO* agrees well with measured *CO* in the left heart ($y = 0.88 x + 13.3$, $n = 104$, $r^2 = 0.93$, SEE = 8.7 $ml \cdot min^{-1} \cdot kg^{-1}$), and right heart ($y = 0.96 x + 5.0$, $n = 104$, $r^2 = 0.88$, SEE = 12.1 $ml \cdot min^{-1} \cdot kg^{-1}$).

Fig. 6. Relationship between predicted and measured values for *CO* (*A*), P_{LA} (*B*) and P_{RA} (*C*) for 128 steps. •, normal cardiac function; ○, left heart failure; dashed line, lines of identity. Prediction was done by intersecting the venous return surface and the integrated cardiac output curve, both of which were estimated from a set of reference hemodynamic values. Regression analysis (solid line) reveals that predicted *CO* ($y=0.93x+6.5$, $n=128$, $r^2 = 0.96$, SEE = 7.5 $ml \cdot min^{-1} \cdot kg^{-1}$), P_{LA} ($y = 0.90 x + 0.5$, $n = 128$, $r^2 = 0.93$, SEE = 1.4 mmHg), and P_{RA} ($y = 0.87 x + 0.4$, $n = 128$, $r^2 = 0.91$, SEE = 0.4 mmHg) agree reasonably well with measured values.

Table 1-1. *Summary of the fit of the relationship between cardiac output and left atrial pressure to 3-parameter logarithmic functions*

Dog No.	S_L	F_L	H_L	r^2	SEE
1	58.1	1.27	0.61	0.98	4.3
2	24.4	2.03	2.71	0.95	3.6
3	108.4	0.00	-0.67	0.95	5.6
4	66.7	2.08	0.08	0.98	5.9
5	105.6	2.30	-0.02	0.99	5.0
6	73.5	2.21	0.59	0.99	2.5
7	42.0	4.32	2.30	0.98	4.7
MEAN (SD)	68.4 (30.9)	2.03 (1.29)	0.80 (1.25)	0.97	4.5 (1.2)

S_L (ml·min^{-1}·kg^{-1}), F_L (mmHg) and H_L (unitless) are the parameters of the logarithmic function for the left heart. See **METHODS** for calculations. r^2, coefficient of determination. SEE, standard error of the estimate (ml·min^{-1}·kg^{-1}).

Table 1-2. *Summary of the fit of the relationship between cardiac output and right atrial pressure to 3-parameter logarithmic functions*

Dog No.	S_R	F_R	H_R	r^2	SEE
1	46.7	2.12	2.34	0.98	4.7
2	33.9	1.50	2.50	0.96	3.3
3	64.1	2.10	2.10	0.90	8.2
4	112.7	1.39	0.19	0.98	5.5
5	101.8	1.39	0.92	0.99	4.6
6	80.6	3.07	1.59	0.99	2.8
7	37.1	3.33	3.69	0.94	6.8
MEAN (SD)	68.1 (31.3)	2.13 (0.8)	1.90 (1.14)	0.96	5.1 (1.9)

S_R (ml·min^{-1}·kg^{-1}), F_R (mmHg) and H_R (unitless) are the parameters of the logarithmic function for the right heart. See **METHODS** for calculations. r^2, coefficient of determination. SEE, standard error of the estimate (ml·min^{-1}·kg^{-1}).

Table 2. *Values of the cardiovascular properties from previously reported data*

HR, beats/min	120
T, min	0.0083
R, mmHg·min·ml^{-1}	0.031
E_{es}, mmHg·ml^{-1}	10
V_0, ml	5
k, ml^{-1}	0.13
α, mmHg	0.25
β, mmHg	4.8
γ (unitless)	1.5

HR, heart rate; *T*, heart period; *R*, systemic arterial resistance ; E_{es}, end-systolic elastance of left ventricle; V_0, volume at which end-systolic pressure is 0 mmHg in left ventricle; k, α, and β, constants characterizing the end-diastolic pressure-volume relationship of the left ventricle; γ, ratio of left ventricular end-diastolic pressure to mean left atrial pressure. See Appendix for abbreviations.

Figure1

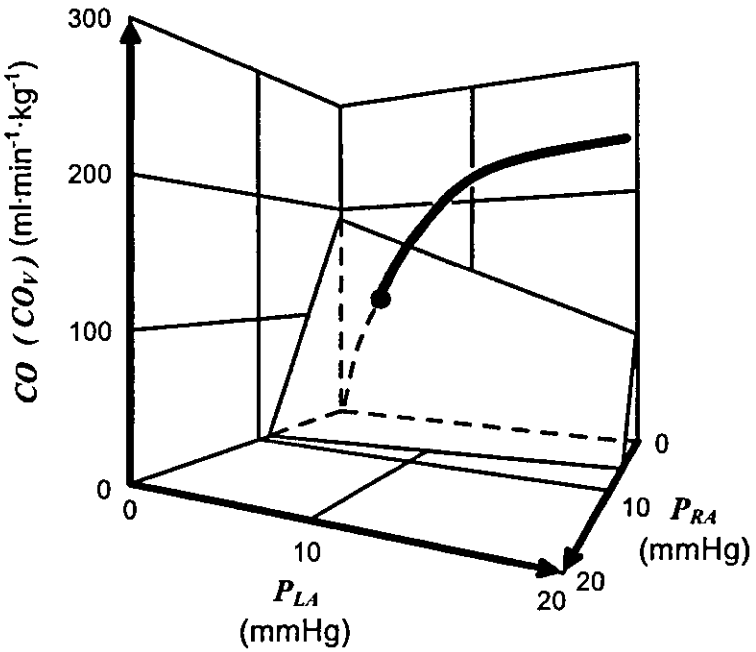

Figure 2

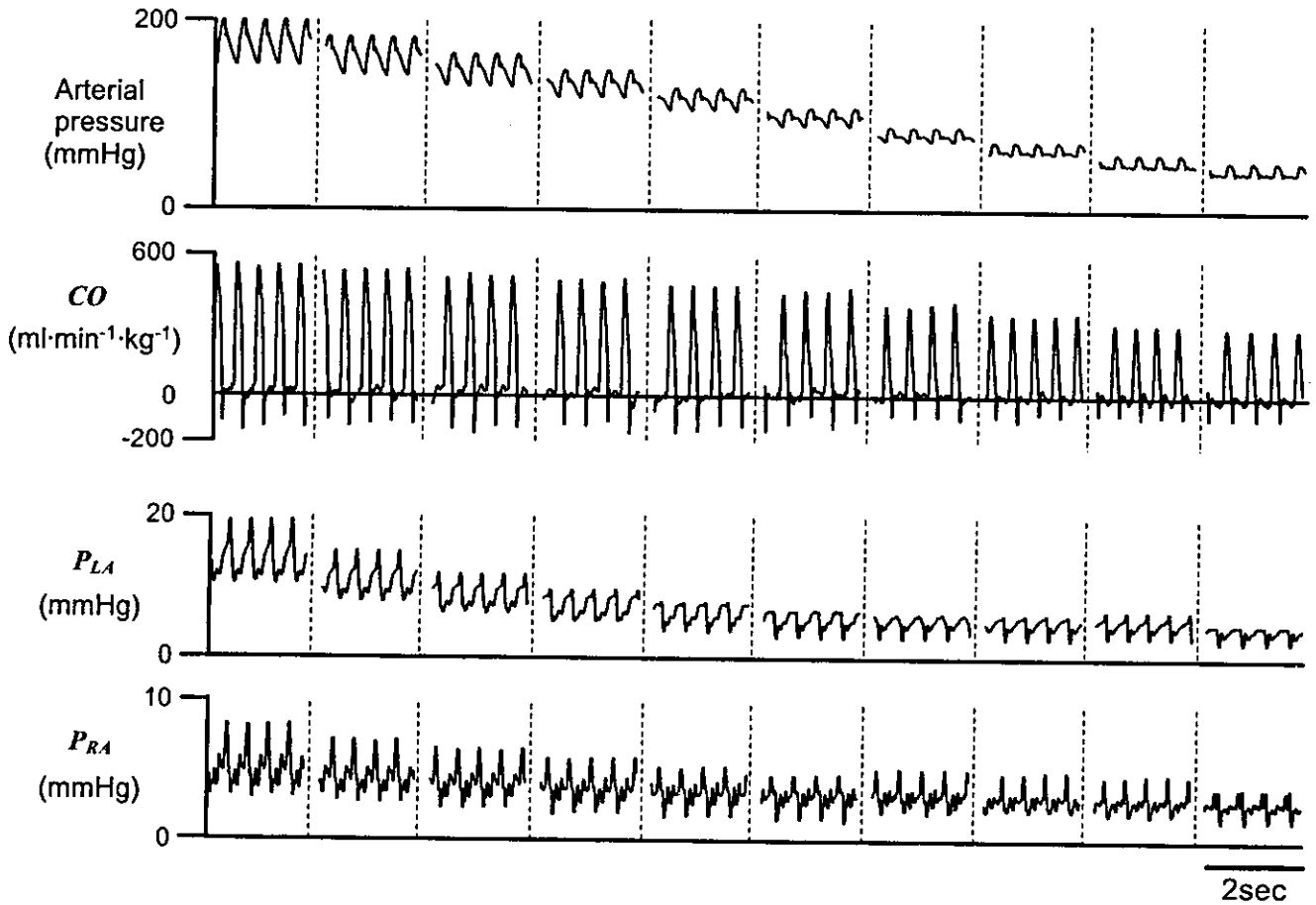
200
Arterial pressure (mmHg)
0
600
CO
(ml·min-1·kg-1)
0
-200
20
PLA
(mmHg)
0
10
PRA
(mmHg)
0
2sec

Figure 3

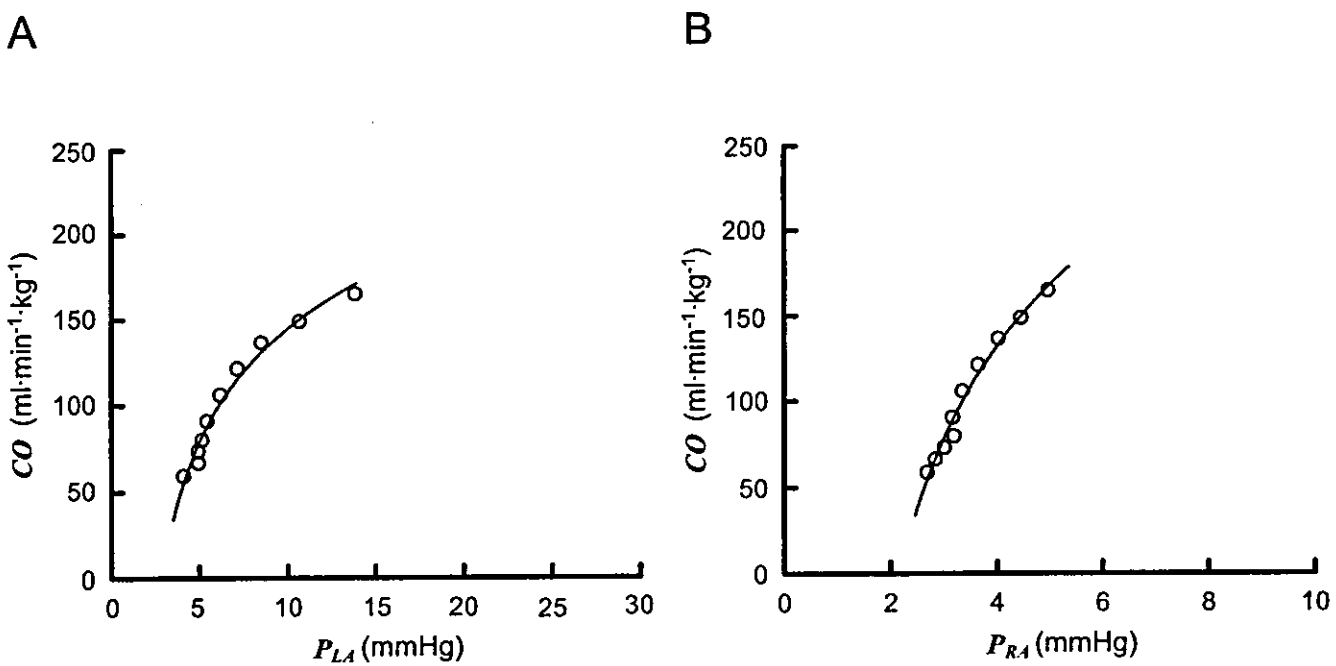
A
B
250
200
150
100
50
0
CO (ml·min-1·kg-1)
0
5
10
15
20
25
30
PLA (mmHg)
0
2
4
6
8
10
PRA (mmHg)

Figure 4

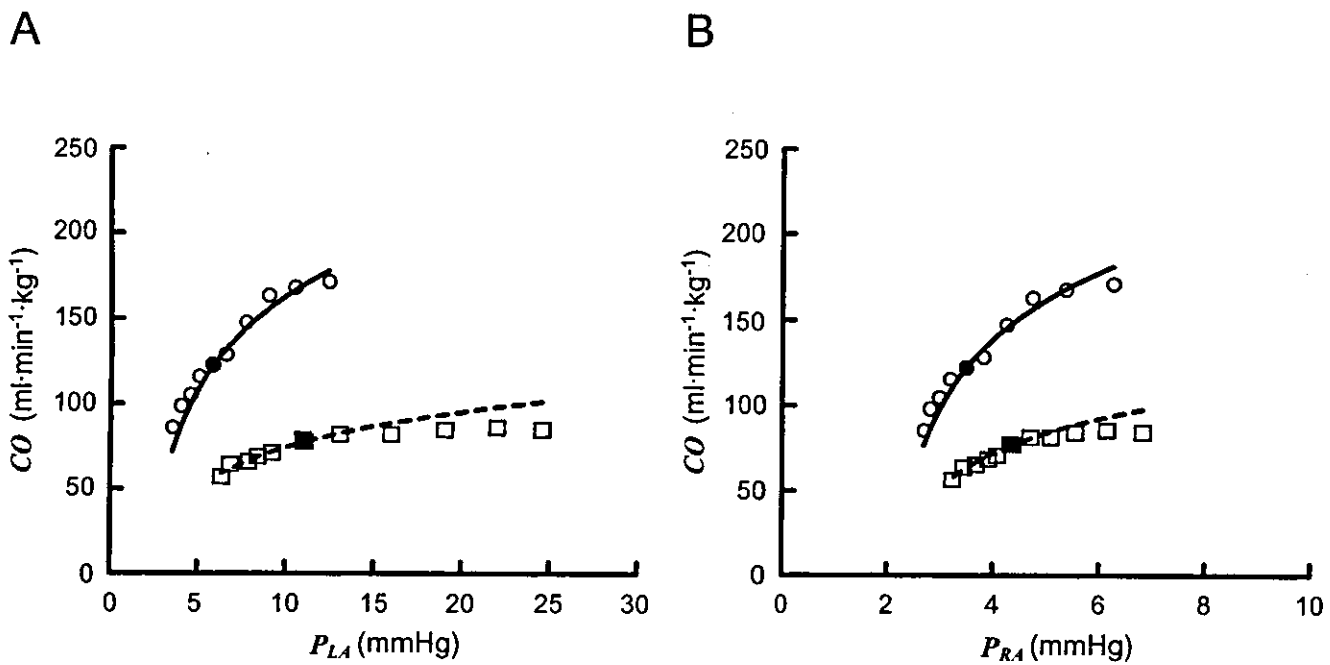
A
B
250
200
150
100
50
0
CO (ml·min⁻¹·kg⁻¹)
0
5
10
15
20
25
30
P_{LA} (mmHg)
0
2
4
6
8
10
P_{RA} (mmHg)

Figure 5

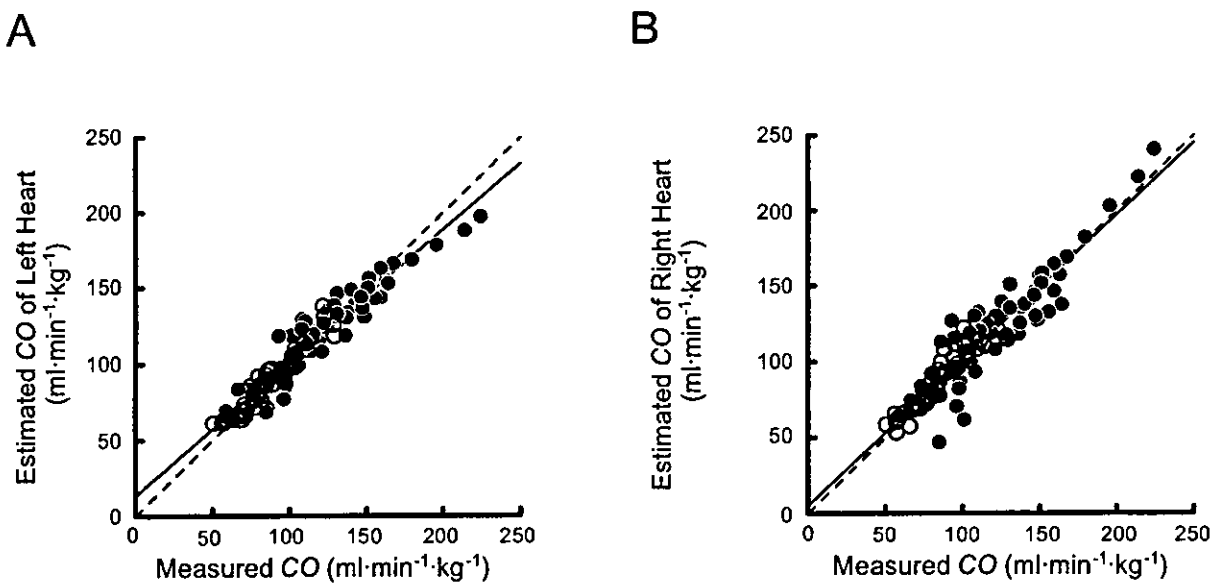
A
B
Estimated CO of Left Heart (ml·min-1·kg-1)
Measured CO (ml·min-1·kg-1)
Estimated CO of Right Heart (ml·min-1·kg-1)
Measured CO (ml·min-1·kg-1)
0
50
100
150
200
250

Figure 6

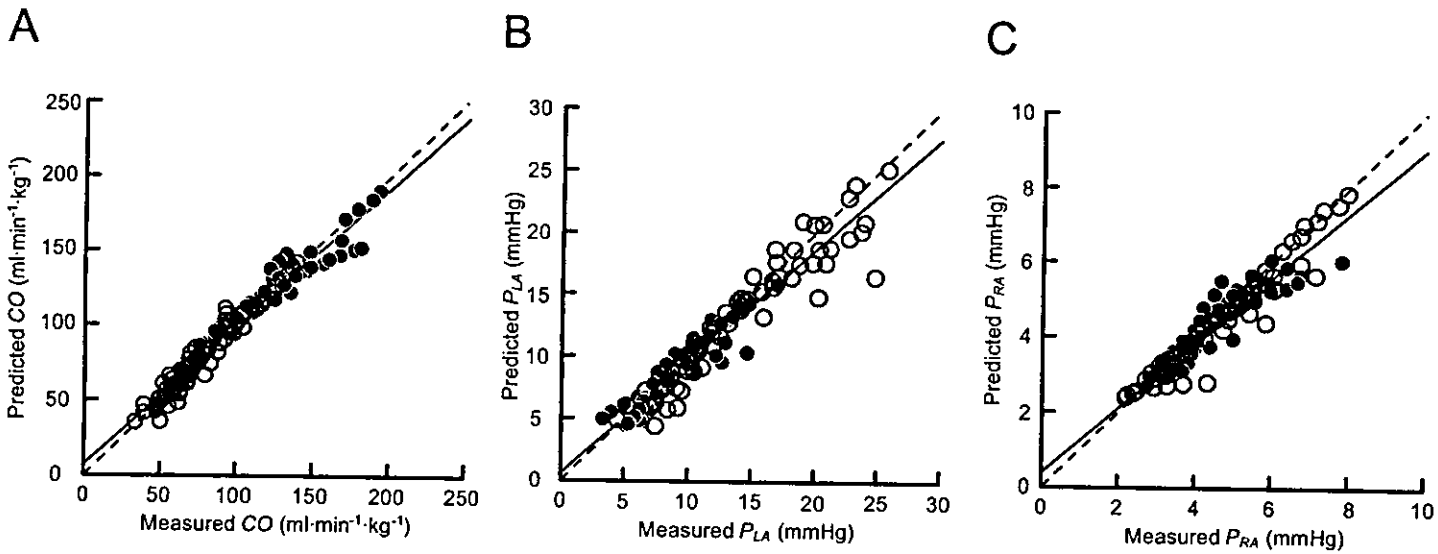
A
B
C
Predicted CO (ml·min⁻¹·kg⁻¹)
Measured CO (ml·min⁻¹·kg⁻¹)
Predicted P_{LA} (mmHg)
Measured P_{LA} (mmHg)
Predicted P_{RA} (mmHg)
Measured P_{RA} (mmHg)

Am J Physiol Heart Circ Physiol 285: H833–H840, 2003.
First published April 24, 2003; 10.1152/ajpheart.01082.2002.

Bezold-Jarisch reflex attenuates dynamic gain of baroreflex neural arc

Koji Kashihara,[1,2] Toru Kawada,[1] Yusuke Yanagiya,[1,2] Kazunori Uemura,[1] Masashi Inagaki,[1] Hiroshi Takaki,[1] Masaru Sugimachi,[1] and Kenji Sunagawa[1]

[1]*Department of Cardiovascular Dynamics, National Cardiovascular Center Research Institute, Suita, Osaka 565-8565; and* [2]*The Organization for Pharmaceutical Safety and Research, Chiyoda-ku, Tokyo 100-0013, Japan*

Submitted 27 December 2002; accepted in final form 21 April 2003

Kashihara, Koji, Toru Kawada, Yusuke Yanagiya, Kazunori Uemura, Masashi Inagaki, Hiroshi Takaki, Masaru Sugimachi, and Kenji Sunagawa. Bezold-Jarisch reflex attenuates dynamic gain of baroreflex neural arc. *Am J Physiol Heart Circ Physiol* 285: H833–H840, 2003. First published April 24, 2003; 10.1152/ajpheart.01082.2002.—Although acute myocardial ischemia or infarction may induce the Bezold-Jarisch (BJ) reflex through the activation of serotonin receptors on vagal afferent nerves, the mechanism by which the BJ reflex modulates the dynamic characteristics of arterial pressure (AP) regulation is unknown. The purpose of this study was to examine the effects of the BJ reflex induced by intravenous phenylbiguanide (PBG) on the dynamic characteristics of the arterial baroreflex. In seven anesthetized rabbits, we perturbed intracarotid sinus pressure (CSP) according to a white noise sequence while renal sympathetic nerve activity (RSNA), AP, and heart rate (HR) were recorded. We estimated the transfer function from CSP to RSNA (neural arc) and from RSNA to AP (peripheral arc) before and after 10 min of intravenous administration of PBG (100 $\mu g \cdot kg^{-1} \cdot min^{-1}$). The intravenous PBG decreased mean AP from 84.5 ± 4.0 to 68.2 ± 4.7 mmHg ($P < 0.01$), mean RSNA to 76.2 ± 7.0% ($P < 0.05$), and mean HR from 301.6 ± 7.7 to 288.4 ± 9.0 beats/min ($P < 0.01$). The intravenous PBG significantly decreased neural arc dynamic gain at 0.01 Hz (1.06 ± 0.08 vs. 0.59 ± 0.17, $P < 0.05$), whereas it did not affect that of the peripheral arc (1.20 ± 0.12 vs. 1.18 ± 0.41). In six different rabbits without intravenous PBG, the neural arc transfer function did not change between two experimental runs with intervening interval of 10 min, excluding the possibility that the cumulative effects of anesthetics had altered the neural arc transfer function. In conclusion, excessive activation of the BJ reflex during acute myocardial ischemia may exert an adverse effect on AP regulation, not only by sympathetic suppression, but also by attenuating baroreflex dynamic gain.

renal sympathetic nerve activity; transfer function; systems analysis; rabbits; carotid sinus baroreflex

THE CIRCULATORY SYSTEM has several mechanoreceptors and chemoreceptors in a variety of regions. The cardiopulmonary region is rich in such receptors. The most vagal afferent fibers from the cardiopulmonary receptors to the vasomotor center are classified as C fibers. Activation of the cardiopulmonary chemosensitive vagal afferent fibers reduces arterial pressure (AP), heart rate (HR), and cardiac output (31). These responses, mediated by 5-hydroxytryptamine (5-HT_3) serotonergic receptors on the cardiopulmonary vagal afferent fibers, are known as the Bezold-Jarisch (BJ) reflex (2, 7, 32). Although its physiological importance remains debatable, the BJ reflex could play a significant role in developing pathological responses associated with acute myocardial ischemia (19, 20, 24). Elucidating the effects of the BJ reflex on the circulatory regulation would be useful for better understanding the pathophysiology of ischemic heart diseases (16, 27). The BJ reflex can be induced chemically with pharmacological agents such as 5-HT and the 5-HT_3 receptor agonist phenylbiguanide (PBG) (31).

In contrast to the BJ reflex, the arterial baroreflex has been established as an important negative feedback system that stabilizes AP against exogenous pressure perturbations. The total baroreflex loop represents the AP response to pressure inputs on the carotid sinuses and aortic baroreceptors. The total baroreflex loop may be divided into the neural and peripheral arc subsystems (6, 22, 25): the neural arc representing signal transduction from baroreceptor pressure input to efferent sympathetic nerve activity (SNA) and the peripheral arc representing the regulatory pathway from SNA to AP. The dynamic characteristics of the two arcs determine the stability and quickness of AP regulation (6, 14). Because the baroreflex operates dynamically under the routine circumstances of daily activity, changes in baroreflex dynamic characteristics would critically affect AP regulation, and consequently the quality of life.

Chen (3) examined the interaction between the BJ and arterial baroreceptor reflexes. In his study, the BJ reflex reduced the steady-state responses of AP and HR to baroreceptor pressure input. However, to the best of our knowledge, the effects of the BJ reflex on the dynamic characteristics of the arterial baroreflex remain unknown. Furthermore, the effects of the BJ reflex on the arterial baroreflex have not been assessed

Address for reprint requests and other correspondence: K. Kashihara, Dept. of Cardiovascular Dynamics, National Cardiovascular Center Research Institute, 5-7-1 Fujishirodai, Suita-shi, Osaka 565-8565, Japan (E-mail: kasihara@ri.ncvc.go.jp).

The costs of publication of this article were defrayed in part by the payment of page charges. The article must therefore be hereby marked "*advertisement*" in accordance with 18 U.S.C. Section 1734 solely to indicate this fact.

separately with regard to the neural and peripheral arc transfer characteristics. Therefore, to test the hypothesis that the BJ reflex modulates the dynamic characteristics of the total loop, neural arc, and/or peripheral arc of the arterial baroreflex, we performed a baroreflex open-loop experiment by using a white noise method in anesthetized rabbits (6, 13, 26). The results of the present study indicate that the BJ reflex evoked by intravenous PBG administration reduced dynamic gain in the total baroreflex loop, mainly by attenuating dynamic gain in the neural arc.

MATERIALS AND METHODS

Surgical Preparations

Animals were cared for in strict accordance with the "Guiding Principles for the Care and Use of Animals in the Field of Physiological Sciences" approved by the Physiological Society of Japan.

Thirteen Japanese white rabbits weighing 2.6–3.0 kg were anesthetized with an injection (2 ml/kg iv) composed of a mixture of urethane (250 mg/ml) and α-chloralose (40 mg/ml). The rabbits were ventilated artificially with oxygen-enriched room air. To maintain the appropriate level of anesthesia, supplemental doses of these anesthetics were administered continuously (0.2–0.3 ml·kg^{-1}·h^{-1} iv). AP was measured using a high-fidelity pressure transducer (Millar Instruments; Houston, TX) inserted from the right femoral artery. A double-lumen catheter was introduced into the right femoral vein for drug administration. We sectioned the aortic depressor nerves after identifying their arterial pulse-synchronized activity to eliminate the effects of the aortic baroreflex. The bilateral vagi were kept intact to preserve the afferent pathway of the cardiopulmonary receptors. We isolated the bilateral carotid sinuses from the systemic circulation by ligating the external and internal carotid arteries and other small branches originating from the carotid sinus regions. The isolated carotid sinuses were filled with warm physiological saline through catheters inserted via the common carotid arteries. Intracarotid sinus pressure (CSP) was controlled with the use of a servo-controlled piston pump. We exposed the left renal sympathetic nerve retroperitoneally and attached a pair of stainless steel wire electrodes (Bioflex wire AS633, Cooner Wire) to record renal SNA (RSNA). The nerve fibers distal to the electrodes were crushed by tight ligature to eliminate afferent signals from the kidney. To insulate and fix the electrodes, and to keep the nerve from drying, the nerve and electrodes were soaked in addition-curing silicone gel (Semicosil 932A/B, Wacker Silicones). The preamplified nerve signal, band-pass filtered at 150–1,000 Hz, was then full-wave rectified and low-pass filtered with a cutoff frequency of 30 Hz to quantify nerve activity. We administered pancuronium bromide (0.3 mg/kg iv) to prevent muscular activity contamination in RSNA recording. Animal body temperature was kept at around 38°C with a heating pad.

Protocols

Protocol 1. After completion of surgical preparations in seven rabbits, the baroreflex negative feedback loop was closed by adjusting CSP to AP for 20 min. Mean AP (and therefore mean CSP) in the steady state was treated as the operating pressure (P_{op}). To assess the dynamic characteristics of the carotid sinus baroreflex, we randomly assigned CSP to either high (P_{op} + 20 mmHg) or low (P_{op} − 20 mmHg) pressure every 500 ms, according to a binary white noise sequence (8–10). The power spectral density of CSP was reasonably constant up to 1 Hz. We recorded CSP, RSNA, AP, and HR for 10 min under control (CTL) conditions. We then administered PBG (100 μg·kg^{-1}·min^{-1} iv) for 20 min and recorded CSP, RSNA, AP, and HR for the last 10 min of the PBG administration (PBG condition).

Protocol 2. To confirm vagi involvement in the PBG-induced BJ reflex, we performed intravenous bolus injection of PBG to six of seven rabbits. After a 30-min recovery period from *protocol 1*, 50 μg iv PBG was injected under the condition of intact vagi. We then sectioned the bilateral vagi and waited until RSNA, AP, and HR reached steady state. Finally, we repeated the bolus injection of PBG under vagotomized condition.

Protocol 3. To examine the time-dependent effects of continuous anesthesia on dynamic characteristics of the arterial baroreflex, we performed an experiment similar to *protocol 1* without intravenous PBG administration in six different rabbits. Data were obtained from two experimental runs of 10 min each (CTL1 and CTL2 conditions) with an intervening interval of 10 min.

Data Analysis

Data were sampled at 200 Hz using a 12-bit analog-to-digital converter and stored on hard disk of a dedicated laboratory computer system. In *protocols 1* and *3*, we estimated the total baroreflex loop transfer function by treating CSP as the input and AP as the output. To estimate neural arc transfer functions of the carotid sinus baroreflex, we treated CSP as input and RSNA as output of the system. In the peripheral arc transfer function, RSNA was the input and AP was the output. We resampled input-output data pairs at 10 Hz and segmented them into eight sets of 50% overlapping bins of 1,024 data points each. A linear trend was subtracted and a Hanning window was applied for each segment. We then performed a fast Fourier transformation to obtain frequency spectra of the input and output signals. We ensemble averaged the input power [$S_{xx}(f)$], output power [$S_{yy}(f)$], and cross power between input and output [$S_{yx}(f)$] over the eight segments, where f represents frequency. Finally, we calculated the transfer function [$H(f)$] from input to output by using the following equation (17)

$$H(f) = \frac{S_{yx}(f)}{S_{xx}(f)} \tag{1}$$

We obtained the modulus [$H(f)$] and phase [$\theta(f)$] of the transfer function using the following equations (17)

$$|H(f)| = \sqrt{H_{Re}(f)^2 + H_{Im}(f)^2} \tag{2}$$

$$\theta(f) = \tan^{-1}\frac{H_{Im}(f)}{H_{Re}(f)} \tag{3}$$

where $H_{Re}(f)$ and $H_{Im}(f)$ are the real and imaginary parts of $H(f)$, respectively. Hereinafter, we denote the modulus as dynamic gain of the transfer function. To quantify the linear dependence between input and output signals in the frequency domain, we calculated a magnitude-squared coherence function [Coh(f)] using the following equation (17)

$$\mathrm{Coh}(f) = \frac{|S_{yx}(f)|^2}{S_{xx}(f)S_{yy}(f)} \tag{4}$$

The coherence value ranges from zero to unity. Unity coherence indicates perfect linear dependence between input and

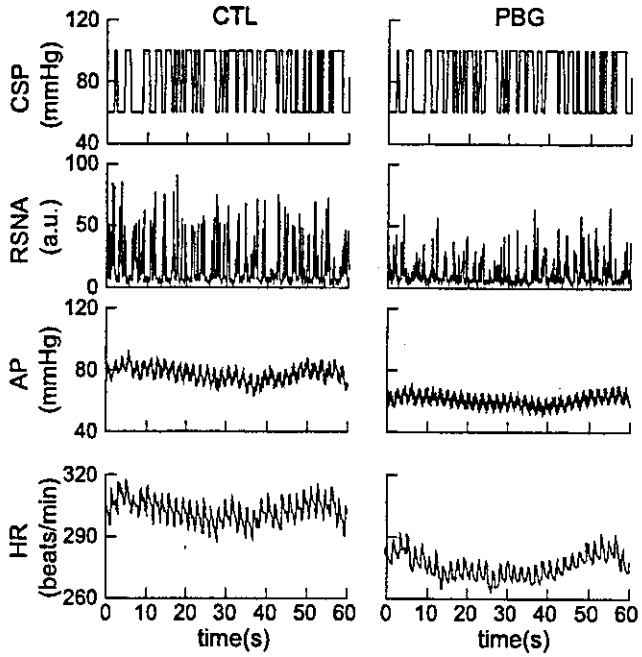

Fig. 1. Typical time series of carotid sinus pressure (CSP), renal sympathetic nerve activity (RSNA), arterial pressure (AP), and heart rate (HR) obtained in the absence (*left*) and presence (*right*) of phenylbiguanide (PBG). CSP was perturbed according to binary white noise sequence; perturbation resulted in RSNA and AP change through baroreflex. a.u., Arbitrary units.

output signals, whereas zero coherence indicates total independence between the two signals.

Statistical Analysis

In *protocol 1*, mean levels of CSP, RSNA, AP, and HR under CTL and PBG conditions were calculated by averaging the respective values for 10 min. Differences in mean levels of CSP, AP, and HR were examined with the use of a paired *t*-test (4). Because RSNA amplitude varied depending on recording conditions, such as physical contact between the nerve and electrodes, the mean level of RSNA was presented as the percent change from control value. Differences in the mean level of RSNA were examined with Wilcoxon's signed-rank test (4).

In *protocol 1*, the transfer function was normalized in each animal so that average gain values <0.03 Hz became unity under the CTL condition. The same normalization factor was applied to the transfer function obtained from the PBG condition. To test the difference between the CTL and PBG conditions, we obtained the gain and phase values at 0.01, 0.1, and 0.5 Hz in each animal. The group differences in these values between the CTL and PBG conditions were examined by paired *t*-test (4). The same analytical procedure was applied to *protocol 3* between CTL1 and CTL2 conditions.

In *protocol 2*, maximum changes in RSNA, AP, and HR were observed within 30 s of the bolus PBG injection. We averaged CSP, RSNA, AP, and HR values for 30 s before and after the PBG injection. Changes in CSP, AP, and HR were examined by paired *t*-test (4). Changes in RSNA were examined by Wilcoxon signed-rank test (4) and are presented as the percent change from the value before the PBG injection. All data are expressed as means ± SE. In all the statistics, differences were considered significant at $P < 0.05$.

RESULTS

Figure 1 shows typical time series of CSP, RSNA, AP, and HR obtained under CTL (*left*) and PBG (*right*) conditions in *protocol 1*. CSP was perturbed according to a binary white noise sequence. Although the CSP sequence was identical between the CTL and PBG conditions in each animal, the binary sequence was changed among the animals. CSP perturbation resulted in RSNA, AP, and HR changes through the carotid sinus baroreflex. PBG administration decreased mean levels of RSNA, AP, and HR compared with the CTL condition.

Figure 2 summarizes mean levels of CSP, RSNA, AP, and HR averaged from the seven rabbits under CTL and PBG conditions in *protocol 1*. Mean levels of CSP were kept unchanged. Mean levels of RSNA, AP, and HR were significantly lower under PBG than under CTL conditions.

Figure 3 shows averaged total baroreflex loop transfer functions under CTL (*left*) and PBG (*right*) conditions in *protocol 1*. Gain, phase, and coherence functions are shown. The gain value at 0.01 Hz approximated unity under the CTL condition, owing to normalization of dynamic gain. The gain decreased as input frequency increased under both CTL and PBG conditions, indicating the low-pass characteristics of the total baroreflex loop. However, the gain under the PBG condition was lower than that under the CTL condition at every frequency. The phase approached $-\pi$ radians at the lowest frequencies, reflecting the negative feedback accomplished by the total baroreflex loop under both CTL and PBG conditions. The coherence was ~0.4 at the lowest frequency, increasing to ~0.7 at the frequencies between 0.04 and 0.8 Hz under the CTL condition. The coherence function in the frequencies between 0.04 and 0.8 Hz was somewhat lower under PBG than under CTL conditions.

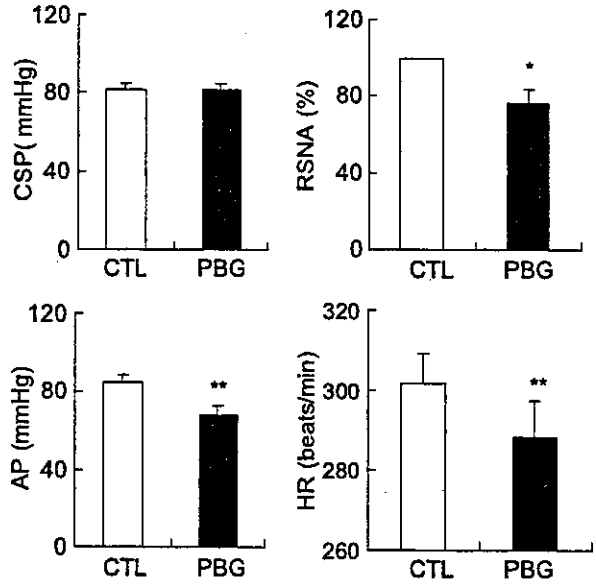

Fig. 2. Mean levels of CSP, RSNA, AP, and HR before and during PBG administration in *protocol 1*. *$P < 0.05$, Wilcoxon signed-rank test; **$P < 0.01$, paired *t*-test. Data are means ± SE.

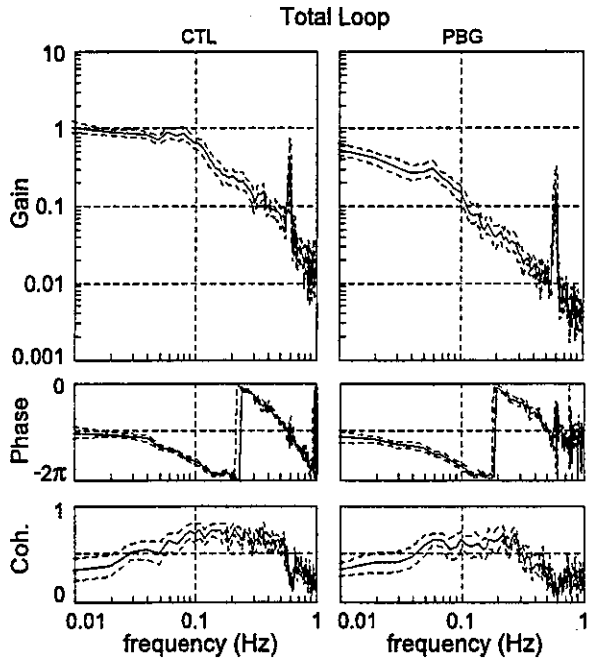

Fig. 3. Total loop transfer functions from CSP to AP averaged from all animals. Gain (U/mmHg), phase (radians), and coherence (Coh.) function under control (CTL) conditions (*left*) and during 100 $\mu g \cdot kg^{-1} \cdot min^{-1}$ PBG administration (*right*) are shown. Solid traces are mean values of transfer functions; dashed traces are means ± SE.

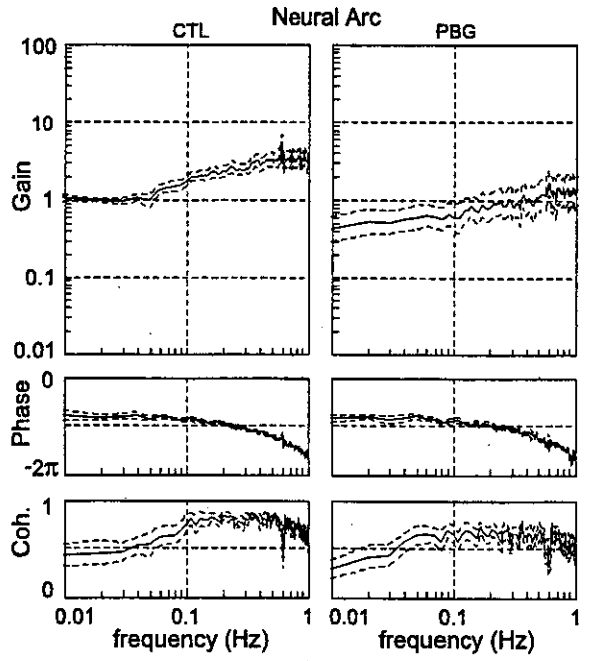

Fig. 4. Transfer functions of neural arc. Averaged gain (U/mmHg), phase (radians), and coherence from CSP to RSNA under CTL (*left*) and 100 $\mu g \cdot kg^{-1} \cdot min^{-1}$ PBG administration (*right*) are shown. Solid and dashed traces represent means ± SE.

Table 1 summarizes the gain and phase values of the total loop transfer functions in Fig. 3. The dynamic gain values were significantly smaller under PBG than under CTL conditions at 0.01, 0.1, and 0.5 Hz. The difference in phase delay between CTL and PBG conditions was significant only at 0.1 Hz.

Table 1. *Parameters of the total loop transfer function from CSP to AP*

	CTL or CTL1	PBG or CTL2
	Protocol 1 (n = 7)	
Gain, U/mmHg		
0.01 Hz	1.19 ± 0.13	0.58 ± 0.11†
0.1 Hz	0.70 ± 0.11	0.17 ± 0.03*
0.5 Hz	0.10 ± 0.03	0.02 ± 0.00†
Phase, radians		
0.01 Hz	−2.95 ± 0.39	−3.66 ± 0.38
0.1 Hz	−5.07 ± 0.21	−5.46 ± 0.24*
0.5 Hz	−8.72 ± 0.18	−9.00 ± 0.16
	Protocol 3 (n = 6)	
Gain, U/mmHg		
0.01 Hz	1.09 ± 0.07	1.06 ± 0.23
0.1 Hz	0.54 ± 0.13	0.47 ± 0.13
0.5 Hz	0.07 ± 0.02	0.06 ± 0.03
Phase, radians		
0.01 Hz	−3.25 ± 0.39	−3.28 ± 0.57
0.1 Hz	−5.40 ± 0.12	−5.32 ± 0.15
0.5 Hz	−8.86 ± 0.32	−9.04 ± 0.37

Values are means ± SE; *n*, no. of rabbits. CSP, carotid sinus pressure; AP, arterial pressure. CTL and PBG represent conditions of control and intravenous phenylbiguanide administration in *protocol 1*, respectively. CTL1 and CTL2 represent the two experimental runs in *protocol 3*. *$P < 0.01$ vs. control; †$P < 0.05$ vs. control.

Figure 4 shows gain, phase, and coherence of the averaged neural arc transfer functions under CTL (*left*) and PBG (*right*) conditions in *protocol 1*. As dynamic gain was normalized, the gain value at 0.01 Hz approximated unity under the CTL condition. The gain values increased as the frequency increased under both CTL and PBG conditions, indicating derivative characteristics of the neural arc. PBG caused an approximately parallel downward shift of the gain plot compared with the CTL condition. The phase value approached $-\pi$ radians at the lowest frequency, reflecting the out-of-phase relationship between CSP and RSNA. The phase plot did not differ between CTL and PBG conditions. The coherence was ~0.4 at the lowest frequency, increasing to ~0.7 at frequencies between 0.04 and 0.8 Hz under the CTL condition. The coherence function under the PBG condition was slightly lower than under the CTL condition.

Table 2 summarizes the gain and phase values of the neural transfer functions shown in Fig. 4. The dynamic gain values were significantly lower under PBG than under CTL conditions at 0.01, 0.1, and 0.5 Hz.

Figure 5 shows gain, phase, and coherence of the averaged peripheral arc transfer functions under CTL (*left*) and PBG (*right*) conditions in *protocol 1*. As the dynamic gain was normalized, the gain value at 0.01 Hz approximated unity under the CTL condition. The dynamic gain values decreased as the input frequency increased under both CTL and PBG conditions, indicating the low-pass characteristics in the peripheral arc. PBG significantly decreased the dynamic gain at 0.1 Hz. The phase approached zero radians at the lowest frequency under both CTL and PBG conditions,

Table 2. *Parameters of the neural arc transfer function from CSP to RSNA*

	CTL or CTL1	PBG or CTL2
	Protocol 1 (n = 7)	
Gain, U/mmHg		
0.01 Hz	1.06 ± 0.08	0.59 ± 0.17†
0.1 Hz	1.80 ± 0.31	0.87 ± 0.24*
0.5 Hz	3.68 ± 0.62	1.72 ± 0.54*
Phase, radians		
0.01 Hz	−2.24 ± 0.35	−2.66 ± 0.26
0.1 Hz	−2.66 ± 0.13	−2.71 ± 0.24
0.5 Hz	−3.77 ± 0.14	−3.59 ± 0.11
	Protocol 3 (n = 6)	
Gain, U/mmHg		
0.01 Hz	1.07 ± 0.07	0.95 ± 0.30
0.1 Hz	1.91 ± 0.15	1.56 ± 0.19
0.5 Hz	4.52 ± 1.07	4.27 ± 0.86
Phase, radians		
0.01 Hz	−2.41 ± 0.46	−2.84 ± 0.64
0.1 Hz	−2.63 ± 0.15	−2.69 ± 0.11
0.5 Hz	−3.54 ± 0.23	−3.39 ± 0.17

Values are means ± SE; *n*, no. of rabbits. RSNA, renal sympathetic nerve activity. CTL and PBG correspond to *protocol 1*. CTL1 and CTL2 correspond to *protocol 3*. *$P < 0.01$ vs. control; †$P < 0.05$ vs. control.

Table 3. *Parameters of the peripheral arc transfer function from RSNA to AP*

	CTL or CTL1	PBG or CTL2
	Protocol 1 (n = 7)	
Gain, U/mmHg		
0.01 Hz	1.20 ± 0.12	1.18 ± 0.41
0.1 Hz	0.45 ± 0.07	0.26 ± 0.06*
0.5 Hz	0.03 ± 0.01	0.02 ± 0.01
Phase, radians		
0.01 Hz	−0.67 ± 0.14	−0.86 ± 0.11
0.1 Hz	−2.43 ± 0.08	−2.66 ± 0.10*
0.5 Hz	−4.95 ± 0.13	−5.23 ± 0.11
	Protocol 3 (n = 6)	
Gain, U/mmHg		
0.01 Hz	1.11 ± 0.07	1.04 ± 0.11
0.1 Hz	0.30 ± 0.05	0.33 ± 0.06
0.5 Hz	0.02 ± 0.00	0.02 ± 0.00
Phase, radians		
0.01 Hz	−0.66 ± 0.09	−0.82 ± 0.16
0.1 Hz	−2.72 ± 0.09	−2.61 ± 0.08
0.5 Hz	−5.33 ± 0.16	−5.50 ± 0.13

Values are means ± SE; *n*, no. of rabbits. CTL and PBG correspond to *protocol 1*. CTL1 and CTL2 correspond to *protocol 3*. *$P < 0.05$ vs. control.

reflecting the fact that a rise in RSNA increased AP. PBG significantly increased phase delay at 0.1 Hz. The coherence values under the CTL condition were from 0.6 to 0.8 at frequencies <0.4 Hz. The coherence values were slightly lower under PBG than under CTL conditions.

Table 3 summarizes the gain and phase values of the peripheral arc transfer functions in Fig. 5. The gain values under the PBG condition were significantly lower than under the CTL condition only at 0.1 Hz.

Figure 6 depicts the results obtained from *protocol 2*. When the vagi were kept intact, PBG significantly decreased RSNA, AP, and HR. RSNA and AP reduc-

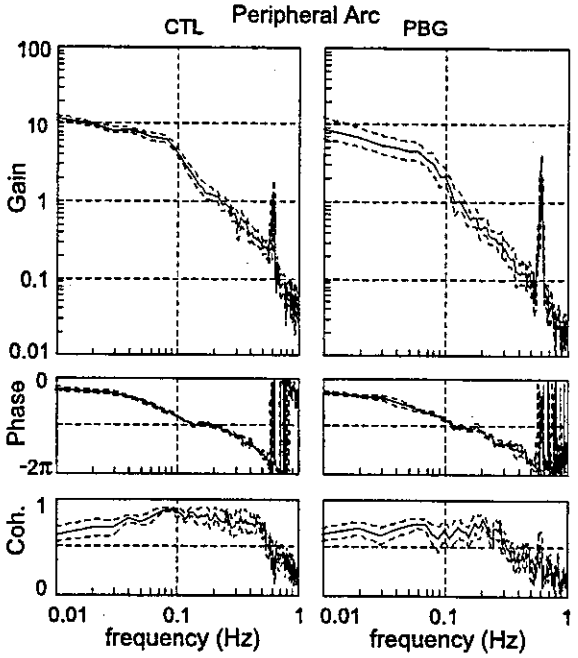

Fig. 5. Transfer functions of effective peripheral arc from RSNA to AP. Averaged gain (U/mmHg), phase (radians), and coherence from RSNA to AP under CTL (*left*) and PBG administration at 100 $\mu g \cdot kg^{-1} \cdot min^{-1}$ (*right*) are shown. Solid traces are mean values of transfer function; dashed traces, ±SE.

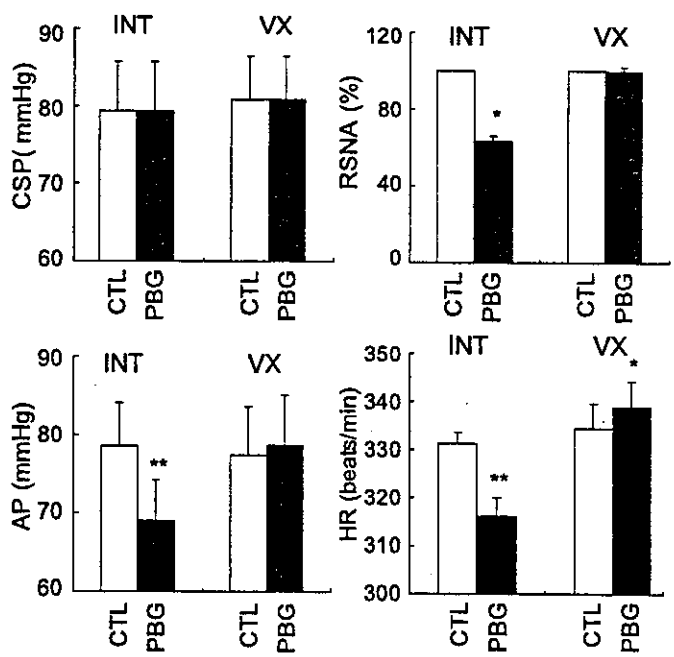

Fig. 6. Mean levels of CSP, RSNA, AP, and HR averaged from six animals before and after bolus PBG injection in *protocol 2*. RSNA, AP, and HR significantly decreased with intact bilateral vagal nerves (INT). RSNA and AP did not change with sectioned bilateral vagal nerves (VX). *$P < 0.05$ vs. control; **$P < 0.01$ vs. control.

tions did not occur after vagotomy. PBG slightly increased HR under the vagotomized condition.

In *protocol 3*, dynamic characteristics of the transfer functions in the total loop, neural arc, and peripheral arc did not differ between CTL1 and CTL2 conditions in all of the frequencies examined (Tables 1–3, *protocol 3*).

DISCUSSION

We have found that intravenous PBG administration attenuated dynamic gain of the total baroreflex loop through a vagal afferent pathway. Separate assessment of the neural and peripheral arc transfer characteristics indicated that the reduction of dynamic gain in the neural arc, rather than in the peripheral arc, was responsible for the PBG-induced attenuation of the total baroreflex gain.

Reduction of Dynamic Gain in Total Baroreflex Loop by BJ Reflex

The open-loop transfer function of the total baroreflex loop shows low-pass characteristics. Intravenous PBG decreased dynamic gain of the total baroreflex loop in every frequency range under study (Fig. 3 and Table 1). The steady-state gain (i.e., dynamic gain at 0.01 Hz) was almost halved by PBG. Although there was a slight difference in phase value between CTL and PBG conditions at 0.1 Hz, the general characteristics of the phase plot were similar between the two conditions. In the following paragraphs we will discuss the transfer function of the total baroreflex loop, focusing on system stability and performance against exogenous perturbations. The absolute gain value of the total baroreflex was, however, left undetermined in the present study because of aortic denervation and possible injury to the carotid sinus nerves during the isolation procedure.

A given negative feedback system could become unstable if its open-loop transfer function showed a gain value greater than unity at a phase value of $-\pi$ radians. A phase delay of $-\pi$ radians was encountered at ~0.2 Hz under the CTL condition in *protocol 1*. It must be noted that a phase value of -2π radians corresponds to a phase delay of $-\pi$ radians in Fig. 3, because the phase value at the lowest frequency is designated as $-\pi$ radians rather than 0 radians, taking into account the negative feedback nature of the total loop. The dynamic gain at 0.2 Hz was approximately one-fifth the steady-state gain. If we simply move the gain plot upward, the steady-state gain of ~5 would make the dynamic gain at 0.2 Hz unity, thereby causing system instability. A previous study (15) indicated that the arterial baroreflex system is marginally stable, suggesting that the absolute gain value of the total baroreflex is ~5. This assumption is based on linear analysis; the actual baroreflex system may only generate sustained oscillation, even with greater gain values, by virtue of system nonlinearity (14). Hosomi et al. (5) reported that the total baroreflex gain estimated from AP response to mild hemorrhage was as great as 7 in rabbits. Because intravenous PBG halved the dynamic gain and increased the gain margin without affecting the phase characteristics, PBG could make the baroreflex system more stable.

One of the important roles of the arterial baroreflex is to attenuate exogenous disturbance on AP. Disturbance minification (m) is calculated from the following equation (21)

$$m = 1/(1 + G) \tag{5}$$

where G represents the total baroreflex gain under the CTL condition. If we assume that intravenous PBG halves the baroreflex gain, minification under the PBG condition can be calculated as

$$m' = 1/(1 + G/2) \tag{6}$$

Dividing *Eq. 6* by *Eq. 5* yields

$$\frac{m'}{m} = \frac{2 + 2G}{2 + G} \tag{7}$$

The ratio of minification is 4/3 when $G = 1$ and asymptotically approaches 2 with increasing G. In other words, the exogenous disturbance affects AP approximately twofold greater under PBG than under CTL conditions. Therefore, the BJ reflex reduces the baroreflex system performance of minification, making AP more vulnerable to exogenous pressure perturbations.

Effects of PBG on Neural and Peripheral Arc Transfer Characteristics

Intravenous PBG decreased the dynamic gain of the neural arc transfer function (Fig. 4), but did not significantly affect that of the peripheral arc transfer function (Fig. 5). Previous studies indicate that the BJ reflex and the arterial baroreflex might share common central pathways, as follows. Autoradiographic studies have shown that most 5-HT_3 receptors in the nucleus tractus solitarius (NTS) are found on the vagal sensory afferent fibers (18). Pires et al. (23) demonstrated that intracisternal or NTS injection of the 5-HT_3 receptor antagonist granisetron significantly attenuated the hypotension and bradycardia evoked by intravenous PBG, suggesting that NTS was involved in the central pathways of the BJ reflex. Verberne et al. (31) demonstrated that barosensitive neurons in the rostral ventrolateral medulla (RVLM) were inhibited by intravenous injection of PBG in rats. It is conceivable that intravenous PBG attenuates the dynamic gain of the neural arc transfer function by affecting baroreflex signal transduction in such brainstem areas as NTS and RVLM through activation of the vagal afferent fibers.

In the present study, mean levels of RSNA were decreased by intravenous PBG. In addition, the RSNA power spectra were reduced by PBG due to decreased dynamic gain of the neural arc transfer function. Notwithstanding differences in the operating point and input power for the peripheral arc, the peripheral arc transfer function differed only at 0.1 Hz between CTL

and PBG conditions (Fig. 5 and Table 3). Also, in a previous study (13), changes in input power did not significantly affect the peripheral arc transfer function. Judging from the static input-output characteristics, the SNA-AP relationship is much more linear than the CSP-SNA relationship (25). Thus the differences in operating point and input power between CTL and PBG conditions would not have been sufficiently large to alter the peripheral arc transfer function.

The total loop transfer function is determined by a product of the neural and peripheral arc transfer functions. The fast neural arc compensated for the slow peripheral arc resulting in the optimization of the dynamic AP regulation in terms of stability and quickness (6). Although dynamic gain of the neural arc was decreased by intravenous PBG compared with the CTL condition, the derivative characteristics of the neural arc were preserved (Fig. 4). In other words, the dynamic gain of the neural arc increased with increasing frequency under both CTL and PBG conditions. As a result, the decreasing slope of dynamic gain in the total loop transfer function was shallower than that in the corresponding peripheral arc transfer function (Figs. 3 vs. 5). However, the total loop gain in every frequency was smaller in PBG than in CTL conditions due to the downward shift of the neural arc transfer function (Fig. 3).

In *protocol 3*, none of the total loop, neural arc, and peripheral arc transfer functions differed between CTL1 and CTL2 conditions (Tables 1–3). Therefore, changes in the transfer functions between CTL and PBG conditions in *protocol 1* were not attributable to the cumulative effects of continuous administration of anesthetics.

Effects of PBG on RSNA, AP, and HR

Intravenous bolus injection of PBG decreased mean levels of RSNA, AP, and HR before vagotomy, which change was erased after vagotomy (Fig. 6). HR was even increased by PBG after vagotomy, suggesting direct action of PBG on the heart. Changes in RSNA and AP during PBG administration are therefore most likely mediated by the activation of vagal afferent fibers. These results were consistent with the study by Veelken et al. (30) where C-fiber activity increased after intravenous PBG administration in rats. The direct actions of PBG on the neural arc and the peripheral arc might have been minimal in the present experimental settings.

Veelken et al. (29) reported that 15-min intravenous injection of PBG decreased RSNA, AP, and HR during the first minute of administration in conscious rats. In their study, only RSNA showed sustained decrease for the 15 min, whereas AP and HR returned to their respective baseline values. In the present study, by contrast, not only RSNA but also AP and HR decreased during PBG administration for 20 min. This apparent contradiction may be partly explained by the difference between baroreflex closed-loop versus open-loop experimental settings. Under baroreflex closed-loop conditions, a decrease in AP is sensed by arterial baroreceptors and the arterial baroreflex counteracts the effects of PBG. Under baroreflex open-loop conditions, counteraction by the arterial baroreflex does not occur, uncovering the pure effects of PBG on the circulatory system. Differences in conscious and anesthetized conditions should also be taken into account.

Clinical Implication

We used intravenous PBG administration to evoke the BJ reflex. Thus the magnitude of the BJ reflex could differ from that induced by myocardial ischemia. However, an increase in the myocardial acetylcholine level induced by intravenous PBG (80 μg/kg) was similar to that observed in the nonischemic myocardium during coronary artery occlusion in anesthetized cats (11, 12). Therefore, the extent of the BJ reflex induced by the present doses of PBG might not be far from that induced by myocardial ischemia. We speculate that the suppression of the arterial baroreflex by the BJ reflex occurs during pathological conditions associated with ischemic heart diseases. To answer the question whether ischemia-induced BJ reflex halves the dynamic gain of the arterial baroreflex, a baroreflex open-loop experiment with coronary artery occlusion should be required.

The induction of the BJ reflex causes bradycardia and hypotension, which may prevent overexertion of cardiac muscle (27). The reduction of energy consumption is considered to be beneficial in hampering ischemic insult. At the same time, however, the BJ reflex blunts the normal AP regulation by the arterial baroreflexes. Because the magnitude of sympathetic inhibition and vagal activation during the BJ reflex is not controlled in terms of systemic AP regulation, excess activation of the BJ reflex could lead to severe bradycardia and hypotension, thereby jeopardizing the patient's life.

Limitations

There are several limitations to this study. First, we performed the experiments using anesthetized rabbits. Because anesthesia affects autonomic nervous activities (28), the results might have been different had we performed the experiment without anesthesia. Second, because the vagi were kept intact, low-pressure baroreflexes from the cardiopulmonary region could interact with the arterial baroreflex, affecting estimation of carotid sinus baroreflex transfer functions. However, the transfer functions estimated in the present study were qualitatively similar to those estimated under vagotomized conditions in previous studies (8–10). We speculate that changes in RSNA, AP, and HR were mainly attributable to CSP input. Third, we filled isolated carotid sinuses with warm physiological saline. Because the ionic content affects baroreceptor sensitivity (1), it might also affect the dynamic characteristics of the neural arc. However, as we did not change the intravascular ionic content in the isolated carotid si-